Optical Gap solitons and Truncated Nonlinear Bloch Waves in Temporal Lattices

Christoph Bersch,[1,2] Georgy Onishchukov,[2] and Ulf Peschel[1]

[1]*Institute of Optics, Information and Photonics, University Erlangen-Nuremberg, Staudtstr. 7/B2, 91058 Erlangen, Germany*
[2]*Max Planck Institute for the Science of Light, Guenther-Scharowsky-Str. 1/B24, 91058 Erlangen, Germany*
(Received 5 June 2012; published 29 August 2012)

We experimentally demonstrate the formation and stable propagation of various types of discrete temporal solitons in an optical fiber system. Pulses interacting with a time-periodic potential and defocusing nonlinearity are shown to form gap solitons and nonlinear truncated Bloch waves. Multipulse solitons with defects, as well as novel structures composed of a strong soliton riding on a weaker truncated nonlinear Bloch wave are shown to propagate over up to eleven coupling lengths. The nonlinear dynamics of all pulse structures is monitored over the full propagation distance which provides detailed insight into the soliton dynamics.

DOI: 10.1103/PhysRevLett.109.093903 PACS numbers: 42.65.Sf, 42.81.Qb

The complex interplay between nonlinearity and periodicity determines the dynamics of many physical systems and leads to the formation of self-localized excitations. These so-called discrete solitons [1,2] are the subject of active research in many areas of physics such as Bose-Einstein condensates [3–5] and nonlinear optics [6]. Nonlinear optical lattices especially provide a prolific environment for exploring the peculiar effects of light propagation in periodic systems [7,8] but have also been envisaged for networking and routing in all-optical circuits [9–11].

Transferring these well-established concepts from space to equivalent systems in the time domain [12] gives access to completely new physical phenomena related to the much richer spectral properties of temporal systems. This may open up fundamentally new possibilities for the engineering of optical communication networks [13,14]. Exploiting the fast fiber nonlinearity paves the way for studying many types of discrete phenomena. The sign of the group velocity dispersion allows us to select between either focusing or defocusing nonlinearity [13].

Recent studies of spatial systems with defocusing nonlinearity confirmed experimentally the existence of stable extended soliton clusters [15–18] which had already been predicted earlier as flat-top solitons [19,20]. For a given set of parameters these truncated nonlinear Bloch waves (TBWs) can occupy an arbitrary number of lattice sites [17] and can take very complex forms [21]; their temporal analogs are archetypes of data patterns in optical telecommunication.

In this Letter, we report on the first experimental observation of discrete temporal solitons. The formation and stable propagation of fundamental gap solitons and truncated nonlinear Bloch waves mediated by a defocusing nonlinearity is demonstrated in a temporal lattice using a recirculating fiber-loop setup. Almost arbitrary bit patterns can be encoded and stabilized by inserting internal defects into a TBW. The stable propagation of these new structures is demonstrated over several coupling lengths. Finally, we study the interaction of a single discrete soliton with a TBW and show experimentally the robust propagation of this new collective state as well as its breakup depending on the power levels of its components. A high-resolution all-optical oscilloscope enables us to measure the soliton dynamics over the complete propagation distance.

We study pulse propagation in a recirculating fiber-loop setup which is typically used to investigate optical long-haul transmission lines in the laboratory. In our case, it consists of several kilometers of single-mode optical fiber with normal group velocity dispersion, an Erbium-doped fiber amplifier to compensate for the loop losses, and a harmonically driven phase modulator [see Fig. 1(b)].

The phase modulation provides a time-periodic potential which is applied discretely once in each loop circulation [14], thereby separating its action from fiber dispersion and nonlinearity, as is illustrated in Fig. 1(a). Here we deal only with a phase modulation much smaller than 2π per round trip. As for guiding-center solitons [22] and numerical split-step algorithms [23], a quasicontinuous model can be applied.

The desired pattern consisting of 25 ps pulses at 10 GHz repetition rate is injected via a 50% coupler into the fiber loop. After each round trip half of the signal continues its propagation inside the loop; the remainder is coupled out for monitoring. The measurements are performed with a linear optical sampling setup [24] which enables us to record the nonlinear evolution of the signal power profile with high temporal resolution over the complete propagation distance. Such a detailed experimental insight into nonlinear pulse propagation in discrete systems is, at present, unattainable in equivalent spatial arrangements [5,6,25].

The propagation of picosecond pulses in our optical fiber system is well described by a modified nonlinear Schrödinger equation [13,23,26]

$$i\partial_Z A - \frac{\beta_2}{2}\partial_T^2 A + \gamma|A|^2 A + V_0 \sin^2(\pi T/T_0) A = 0, \quad (1)$$

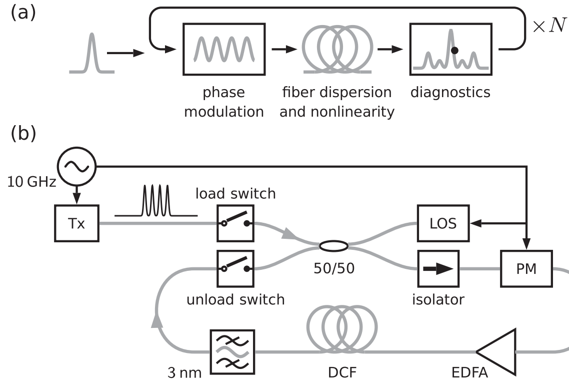

FIG. 1. (a) Illustration of the experimental separation of phase modulation from fiber effects. (b) Block scheme of the experimental setup. A transmitter (Tx) generates patterns of 25 ps pulses with 10 GHz pulse repetition rate at 1550 nm. Acousto-optic load and unload switches control the loop operation. In each circulation a high-frequency periodic phase modulation (PM) is imposed on the pulses which are subsequently amplified with an Erbium-doped fiber amplifier (EDFA) before entering a dispersion-compensating fiber [DCF, $L = 1.4$ km, $\gamma = 7(\mathrm{W\,km})^{-1}$, $\beta_2 = 120$ ps^2/km, the total dispersion of all other components can be neglected; see text for definitions]. An optical bandpass filter removes excess noise from the signal. The fiber loop circulation time is synchronized with the 10 GHz microwave signal applied to the phase modulator. The pulse propagation is monitored with a high-resolution linear optical sampling setup (LOS).

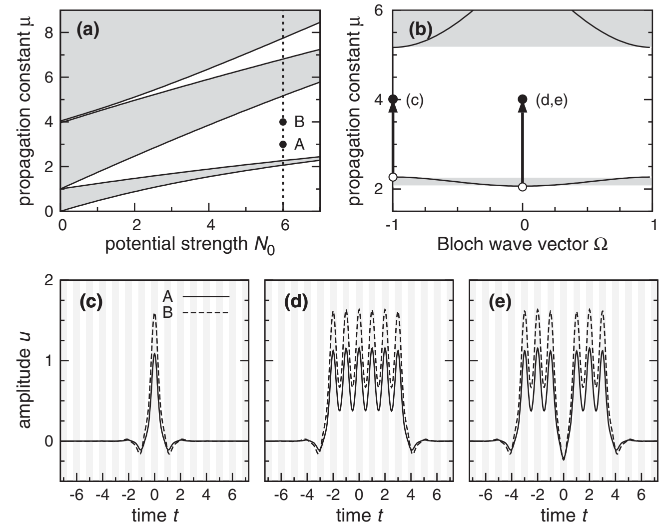

FIG. 2. (a) Dependence of the linear transmission bands (shaded) on the potential depth N_0. (b) Bifurcation behavior of the numerical soliton solutions [35] in (c)–(e) with respect to the band structure of Bloch waves (Ω: normalized Bloch vector). (c) Fundamental gap soliton, (d) a six-peak TBW, and (e) a six-peak TBW with defect. The soliton solutions are shown for a fixed potential strength $N_0 = 6$ at propagation constants $\mu = 3.0$ (solid line) and $\mu = 4.0$ (dashed line), which are also marked in the band structure (a) as A and B, respectively.

where $T = t_{\mathrm{lab}} - Z/v_g$ is time in the reference frame comoving with the pulse envelope A at its group velocity v_g and Z is the propagation coordinate. V_0 is the amplitude of an effective time-periodic potential with period T_0 which depends on the phase modulation depth Φ_0 and the length of the loop L_0 as $V_0 = \Phi_0/L_0$. β_2 is the group-velocity dispersion (GVD), and γ the Kerr nonlinearity of the fiber (see Fig. 1 for the experimental parameters). Normalizing Eq. (1) to characteristic scales gives us

$$i\partial_z U - \sigma\partial_t^2 U + |U|^2 U + N_0 \sin^2(t) U = 0, \qquad (2)$$

where $t = \pi T/T_0$, $z = Z/Z_0$ with $Z_0 = 2T_0^2/(\pi^2|\beta_2|)$, $U = \sqrt{Z_0\gamma}A$, and the potential strength is scaled as $N_0 = Z_0 V_0$. The coupling between the sites of the temporal lattice is facilitated by the GVD and can be positive ($\sigma = +1$) for normal or negative ($\sigma = -1$) for anomalous dispersion, in contrast to analogous spatial systems where diffraction restricts the coupling to positive values. For normal GVD as studied here, Eq. (2) is equivalent to well-investigated spatial systems with defocusing nonlinearity [6,17].

Equation (2) supports stationary solitary wave solutions of the form $U(z, t) = u(t)\exp(i\mu z)$. Among them are clusters known as flat-top solitons or TBWs [16,17,19,20] which can be viewed as a composition of fundamental gap solitons [27]. Figure 2(b) illustrates the bifurcation behavior of the solitons with respect to the band structure of Bloch waves. TBWs like the one shown in Fig. 2(d) do not bifurcate from the first band like fundamental gap solitons, but when the power is increased the defocusing nonlinearity shifts them out of the first band before they localize in the first band gap [16–18]. A TBW which features an internal defect, as is displayed in Fig. 2(e), belongs to a different soliton family as it has a distinct topological structure. All these soliton compositions can be excited experimentally as we will demonstrate in the following. Solitons residing in other band gaps [27] or for anomalous dispersion do also exist [20] and are also expected to be accessible experimentally. All the created localized structures are completely immobile and localize on individual lattice sites. This is different from the gap solitons observed in Bragg gratings, which cover hundreds of unit cells and can even move across the lattice.

Typical experimental results for the linear and nonlinear evolution of single pulses are illustrated in Fig. 3. Without any phase modulation the pulses spread quickly, as can be seen in Fig. 3(a), a process which is even accelerated by the nonlinearity of the fiber [23]. As soon as the phase modulation is switched on, the fields become localized at the phase minima and the spreading slows down considerably. This discrete temporal diffraction [14] is equivalent to its spatial counterpart observed in waveguide arrays. Using the maximum pulse spreading angle $\alpha_{\max}$ in the linear case, Fig. 3(b), we estimated the coupling length [28] to be $L_{\mathrm{cpl}} \approx T_0\pi/\alpha_{\max} \approx 500$ km for a phase modulation

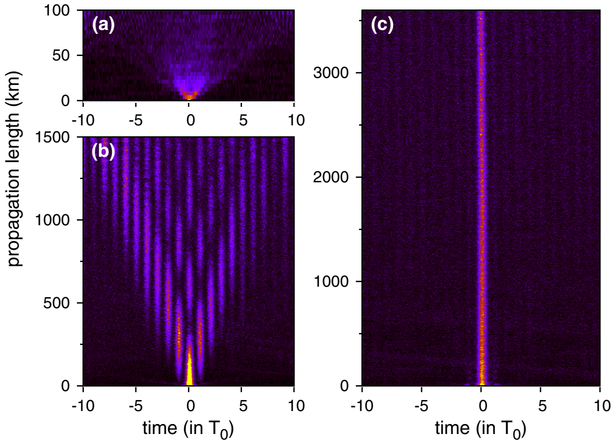

FIG. 3 (color online). Linear and nonlinear evolution of a single pulse. (a) Nonlinear pulse broadening without periodic potential and 30 mW pulse peak power. (b) The discrete diffraction of the pulse in the temporal lattice for low power (500 μW) and (c) the discrete soliton with 30 mW pulse peak power. In both cases the phase modulation depth is 0.5 rad ($N_0 = 6$).

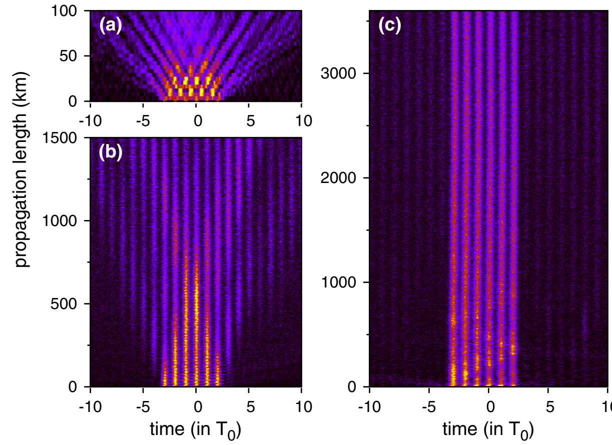

FIG. 4 (color online). Linear and nonlinear evolution of a six-peak pulse sequence. (a) Nonlinear broadening without temporal potential. The linear evolution with the lattice and the resulting discrete diffraction pattern is shown in (b). The formation and stable propagation of truncated nonlinear Bloch waves can be seen in (c). All parameters are as indicated in Fig. 3.

depth of $\Phi_0 = 0.5$ rad corresponding to a potential strength of $N_0 = 6$ in the continuous model [Eq. (2)]. This value for the potential strength is used for all measurements presented in this Letter. The input pulses for the linear propagation shown in Fig. 3(b) have a peak power of 500 μW. All power values are given as peak powers and are averaged over the fiber length of one loop round trip to take into account the fiber losses.

When increasing the power the propagation constant μ of the field enters the first band gap and a fundamental gap soliton forms. For 30 mW the soliton is already localized deep inside the gap [see Fig. 3(c)]. Note that this soliton peak power is orders of magnitude smaller than for any other optical system supporting discrete solitons based on a fast nonlinearity [6]. We would like to emphasize that the bright solitons form in a regime with a strong normal GVD, which even enhances the nonlinear pulse spreading in the absence of a supporting periodic potential, as can be seen in Fig. 3(a).

We could demonstrate stable soliton propagation over a distance of 3500 km (2500 loop round trips) corresponding to seven coupling lengths, as is demonstrated in Fig. 3(c). As each round trip incorporates an amplification process, noise is added in the form of amplified spontaneous emission to the signal. Although this should also result in Gordon-Haus timing jitter of the signal pulses [29,30], measurements like those displayed in Fig. 3(c) do not show noteworthy timing fluctuations. This can be explained from two distinct perspectives: from the viewpoint of discrete dynamics, fundamental gap solitons are transversely immobile [6,31] which manifests as timing stabilization in our setup. From a more technical perspective, our experimental arrangement reminds us of synchronous modulation as is used for retiming in all-optical regenerators [32]. Still, the accumulation of amplified spontaneous emission from optical amplifiers represents a major limitation for the achievable propagation distance.

The optical transmitter allows us to generate and propagate arbitrary bit patterns at 10 GHz pulse repetition rate which is employed to study truncated nonlinear Bloch waves. Figure 4 shows experimental results after launching a sequence of six in-phase pulses into the fiber loop. Their linear propagation inside the lattice results in spreading of the initial distribution because of evanescent coupling. The maximum spreading angle imposed by the periodic potential is clearly visible in Fig. 4(b). The nonlinear evolution in the presence of the temporal lattice gives rise to stable TBWs, as can be seen in Fig. 4(c). The experimental parameters are the same as for the fundamental gap soliton in Fig. 3.

Moving toward more complex soliton states, we study the evolution of different multipulse patterns featuring internal defects. When a single defect is introduced into the six-peak pattern of Fig. 4, the resulting pulse sequence stays unchanged upon nonlinear propagation in the temporal lattice [Fig. 5(a)]. This defect TBW is not a combination of two three-peak solutions but belongs to a distinct soliton family (see, e.g., Ref. [1]). Figure 5(b) shows the realization of another kind of defect TBW which features two single defects separated by two lattice sites. These two patterns are representatives of arbitrary bit patterns which can form solitons in the system.

From the perspective of our temporal approach, the existence of these distinct TBW families is equivalent to the nonlinear stabilization of arbitrary bit patterns with on-off keying, thus suggesting potential applications in optical communication. Contrary to common soliton transmission [30], the duty cycle of the pulses in a TBW is very high, about 50%. This value is close to that used in modern transmission systems with return-to-zero modulation

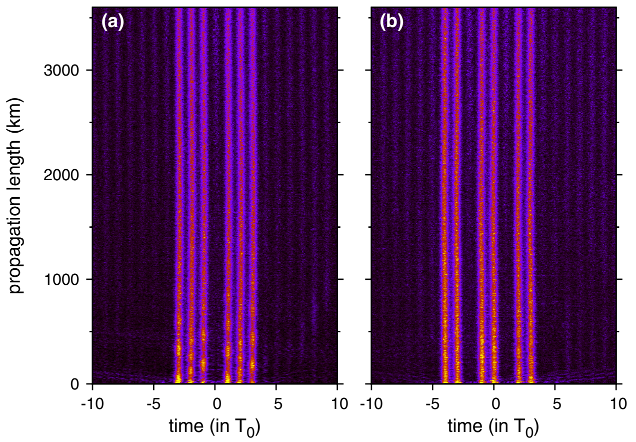

FIG. 5 (color online). Nonlinear evolution of two pulse patterns with one (a) or two (b) single internal defects for $\hat{P} = 30$ mW and $N_0 = 6$. The patterns form defect TBWs which are stable for over 3500 km.

formats. The spectral efficiency of TBWs is very high because their spectrum is as narrow as that of single solitons.

Potentially, our system is not limited to binary on-off formats. Multipulse patterns featuring a single peak with a power higher than the surrounding TBW can also be launched. The nonlinear propagation and in particular the robustness of such multilevel structures is expected to depend critically on the power ratio.

Figure 6(a) displays the nonlinear evolution of such a novel structure consisting initially of a strong central pulse having $r = 2.5$ times the 20 mW peak power of the surrounding TBW. The strong peak distributes its energy over the surrounding pulses and completely disappears after only a few loop circulations. An isolated pulse of the same power of 50 mW would immediately form a gap soliton as can be deduced from Fig. 3(c). For these power levels the propagation constants of the fundamental gap soliton and the TBW are too close, such that phase matching causes an efficient energy transfer between them during propagation. It is worth noting that still all the power remains confined to the initially excited seven lattice sites which somehow form a kind of nonlinear background completely decoupled from the rest of the lattice.

Increasing the power ratio leads to an efficient decoupling of the single pulse from the background TBW. A typical measurement with $r = 4$ (single pulse power of 60 mW, TBW power of 15 mW) is shown in Fig. 6(b) which clearly demonstrates that the composition of a TBW with a "piggyback" gap soliton maintains its initial shape for at least 5600 km, which corresponds to eleven coupling lengths. This is even more surprising because the coexistence of these two solitary structures with different propagation constants results in a nonstationary, but nevertheless well-localized state. This is the first time, to our knowledge, that the stable propagation of such a structure has been observed.

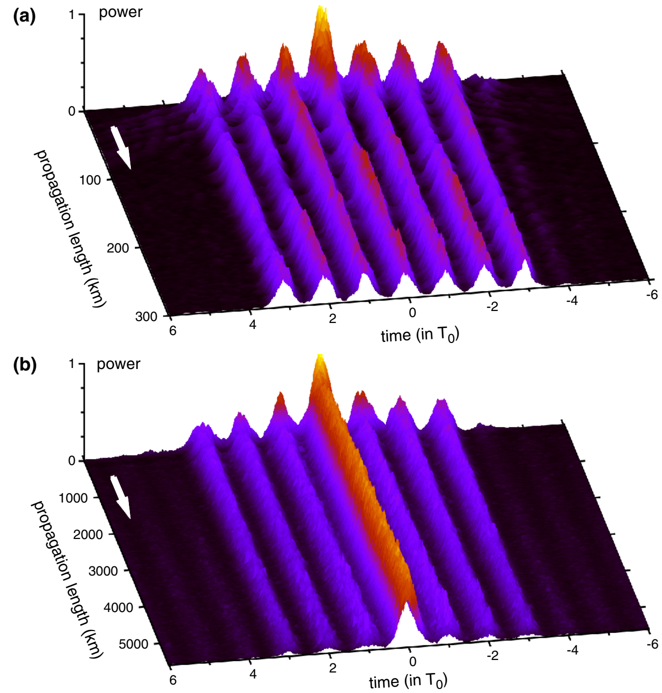

FIG. 6 (color online). Measurement of the nonlinear evolution of two pulse patterns consisting of seven peaks, with the central one having a peak power higher than the surrounding TBW. For a power ratio $r = 2.5$, the central pulse couples to the underlying TBW and decays (a). Its propagation is shown for only 300 km to visualize the breakup. An increased power ratio of $r = 4$ leads to an effective decoupling of the two solitons and the input pulse structure stays unchanged for at least 5600 km (b).

In conclusion, we have demonstrated the formation of temporal solitary structures in an effectively time-discretized optical fiber system. The interplay of a fast nonlinearity and a time-periodic potential was employed to observe temporal gap solitons as well as truncated nonlinear Bloch waves with and without internal defects. The pulse propagation at milliwatt peak powers with defocusing nonlinearity was monitored with high temporal resolution over up to eleven coupling lengths. Finally, we reported on the joint propagation of a truncated nonlinear Bloch wave with a "piggyback" gap soliton. It was demonstrated that this novel structure is robust for an appropriate choice of optical power. The attained symbiosis of discrete optics and fiber-based optical communications not only sheds new light on long-known techniques like synchronous modulation [32], active optical buffering [33], and ultra-long-haul optical data transmission [34], but also indicates new possibilities for all-optical signal processing.

The authors acknowledge fruitful discussions with A. Regensburger and financial support by the Deutsche Forschungsgemeinschaft (Research Unit 532 and Cluster of Excellence Engineering of Advanced Materials) and the German-Israeli Foundation.

[1] S. Flach and A. V. Gorbach, Phys. Rep. **467**, 1 (2008).
[2] D. K. Campbell, S. Flach, and Y. S. Kivshar, Phys. Today **57**, 1, 43 (2004).
[3] A. Trombettoni and A. Smerzi, Phys. Rev. Lett. **86**, 2353 (2001).
[4] B. Eiermann, T. Anker, M. Albiez, M. Taglieber, P. Treutlein, K.-P. Marzlin, and M. K. Oberthaler, Phys. Rev. Lett. **92**, 230401 (2004).
[5] O. Morsch and M. Oberthaler, Rev. Mod. Phys. **78**, 179 (2006).
[6] F. Lederer, G. I. Stegeman, D. N. Christodoulides, G. Assanto, M. Segev, and Y. Silberberg, Phys. Rep. **463**, 1 (2008).
[7] A. A. Sukhorukov, Y. S. Kivshar, H. S. Eisenberg, and Y. Silberberg, IEEE J. Quantum Electron. **39**, 31 (2003).
[8] D. N. Christodoulides, F. Lederer, and Y. Silberberg, Nature (London) **424**, 817 (2003).
[9] A. B. Aceves, C. De Angelis, T. Peschel, R. Muschall, F. Lederer, S. Trillo, and S. Wabnitz, Phys. Rev. E **53**, 1172 (1996).
[10] D. Neshev, A. A. Sukhorukov, B. Hanna, W. Krolikowski, and Y. S. Kivshar, Phys. Rev. Lett. **93**, 083905 (2004).
[11] R. Keil, M. Heinrich, F. Dreisow, T. Pertsch, A. Tunnermann, S. Nolte, D. N. Christodoulides, and A. Szameit, Sci. Rep. **1**, 94 (2011).
[12] E. Treacy, IEEE J. Quantum Electron. **5**, 454 (1969).
[13] U. Peschel, C. Bersch, and G. Onishchukov, Central Eur. J. Phys. **6**, 619 (2008).
[14] C. Bersch, G. Onishchukov, and U. Peschel, Appl. Phys. B **104**, 495 (2011).
[15] T. Anker, M. Albiez, R. Gati, S. Hunsmann, B. Eiermann, A. Trombettoni, and M. K. Oberthaler, Phys. Rev. Lett. **94**, 020403 (2005).
[16] T. J. Alexander, E. A. Ostrovskaya, and Y. S. Kivshar, Phys. Rev. Lett. **96**, 040401 (2006).
[17] J. Wang, J. Yang, T. J. Alexander, and Y. S. Kivshar, Phys. Rev. A **79**, 043610 (2009).
[18] F. H. Bennet, T. J. Alexander, F. Haslinger, A. Mitchell, D. N. Neshev, and Y. S. Kivshar, Phys. Rev. Lett. **106**, 093901 (2011).
[19] S. Darmanyan, A. Kobyakov, F. Lederer, and L. Vázquez, Phys. Rev. B **59**, 5994 (1999).
[20] T. Alexander and Y. Kivshar, Appl. Phys. B **82**, 203 (2006).
[21] T. J. Alexander, Phys. Rev. A **83**, 043624 (2011).
[22] A. Hasegawa and Y. Kodama, Phys. Rev. Lett. **66**, 161 (1991).
[23] G. P. Agrawal, *Nonlinear Fiber Optics* (Academic, New York, 1995), 4th ed.
[24] C. Dorrer, D. Kilper, H. Stuart, G. Raybon, and M. Raymer, IEEE Photonics Technol. Lett. **15**, 1746 (2003).
[25] C. Barsi, W. Wan, and J. W. Fleischer, Nature Photon. **3**, 211 (2009).
[26] S. Wabnitz, Electron. Lett. **29**, 1711 (1993).
[27] Y. Zhang and B. Wu, Phys. Rev. Lett. **102**, 093905 (2009).
[28] H. S. Eisenberg, Y. Silberberg, R. Morandotti, and J. S. Aitchison, Phys. Rev. Lett. **85**, 1863 (2000).
[29] J. P. Gordon and H. A. Haus, Opt. Lett. **11**, 665 (1986).
[30] Y. Kivshar and G. Agrawal, *Optical Solitons: From Fibers to Photonic Crystals* (Academic Press, New York, 2003).
[31] A. B. Aceves, C. De Angelis, S. Trillo, and S. Wabnitz, Opt. Lett. **19**, 332 (1994).
[32] Z. Zhu, M. Funabashi, Z. Pan, L. Paraschis, and S. Yoo, IEEE Photonics Technol. Lett. **18**, 718 (2006).
[33] D. J. Jones, K. L. Hall, H. A. Haus, and E. P. Ippen, Opt. Lett. **23**, 177 (1998).
[34] M. Nakazawa, E. Yamada, H. Kubota, and K. Suzuki, Electron. Lett. **27**, 1270 (1991).
[35] J. Yang and T. I. Lakoba, Stud. Appl. Math. **118**, 153 (2007).